3D Helix Engineering in Chiral Photonic Materials

Kragt, Augustinus J.J.; Hoekstra, Davey C.; Stallinga, Sjoerd; Broer, Dirk J.; Schenning, Albertus P.H.J.

Important note
To cite this publication, please use the final published version (if applicable).
Please check the document version above.

3D Helix Engineering in Chiral Photonic Materials

Augustinus J. J. Kragt, Davey C. Hoekstra, Sjoerd Stallinga, Dirk J. Broer, and Albertus P. H. J. Schenning*

Engineering the helical structure of chiral photonic materials in three dimensions remains a challenge. 3D helix engineered photonic materials are fabricated by local stratification in a photopolymerizable chiral nematic liquid crystal. The obtained chiral photonic materials reflect both handedness of circular polarized light and show super-reflectivity. Simulations match the experimentally observed photonic properties and reveal a distorted helical structure. 3D engineered polymer films can be made that reflect both left- and right handed circular and linear polarized light dependent and exhibit a changing color contrast upon altering the polarization of incident light. Hence, these 3D engineered photonic materials are of interest for new and emerging applications ranging from anti-counterfeit labels and data encryption to aesthetics and super-reflective films.

Nature provides a library of complex 3D photonic architectures with unique polarization-dependent photonic properties and exceptional decorative function.[1–8] For example, the exocuticle of the beetle *Chrysina gloriosa* is partly decorated with a brilliant metallic color, which selectively reflects left circularly polarized (LCP) light due to helicoidally arranged nested arcs.[1,3,9] Other animals, such as the butterfly *Papilio blumei*, show linear polarized (LP) light selectivity on specific parts of their wings.[3,4,10] Natural 3D photonic structures have inspired researchers to fabricate complex architectures to make products with appealing aesthetics and distinctive polarization-dependent decorations, such as security features.[3–8,11–20]

Synthetic photonic structures that only reflect left- or right-handed circular polarized (CP) light are chiral nematic liquid crystals (LCs).[1,3] In a chiral nematic LC, the molecular directors of consecutive liquid crystal planes are rotated with respect to each other in a helical fashion. This results in a periodic directional variation of the extraordinary and ordinary refractive indices (n_e and n_o, respectively), giving rise to Bragg reflection.

Due to the helical structure, the reflection is not linear polarized light dependent and only circularly polarized light with the same handedness as the helical structure is reflected. As a result, the reflectivity of unpolarized light is limited to 50%.[21–23]

By helix engineering in the *z*-direction, along the film thickness, the photonic properties of chiral nematic LCs can be altered. Both handedness of CP light can be reflected by helix inversion or wash-and-refill methods in polymer-stabilized low molecular weight LC systems, thereby exceeding the 50% reflection limit of unpolarized light.[24–29] For chiral nematic LC polymers, multilayer stacks can be fabricated consisting of layers reflecting the opposite handedness or layers of the same handedness separated by half-wave plates.[24,30,31] An LP light dependency can be introduced by stratification of chiral and nonchiral components. This deforms the helical structure and causes a net excess of molecules to be oriented in one direction.[32] However, helix engineering in three dimensions, both along the helix and in the *x–y* plane, in a single photonic polymer with programmed super-reflectivity and LP light dependency remains a challenge.

In this work, we engineered the helical structure of chiral nematic LC materials in three dimensions. Engineering along the *z*-direction was done by stratification of an uncrosslinked LC elastomer (LCE) and a chiral LC network (LCN) on the pitch length scale (hundreds of nanometers), while engineering in the *x–y* plane was achieved by photomask exposure, thereby localizing the stratification to a macrosized region.[33] The stratified polymer coatings reflect both handedness of CP light, thereby exceeding the 50% reflection limit for unpolarized light of regular chiral nematic LCs. In addition, the stratified polymer reflects both CP and LP light dependent, whereas the

A. J. J. Kragt, D. C. Hoekstra, Prof. D. J. Broer, Prof. A. P. H. J. Schenning
Stimuli-responsive Functional Materials and Devices
Department of Chemical Engineering and Chemistry
Eindhoven University of Technology
Den Dolech 2, 5600 MB Eindhoven, The Netherlands
E-mail: a.p.h.j.schenning@tue.nl

A. J. J. Kragt, Prof. D. J. Broer, Prof. A. P. H. J. Schenning
SCNU-TUE Joint Laboratory of Device Integrated Responsive
Materials (DIRM)
South China Normal University
Guangzhou Higher Education Mega Center
510006, Guangzhou, China

A. J. J. Kragt, D. C. Hoekstra, Prof. D. J. Broer, Prof. A. P. H. J. Schenning
Institute for Complex Molecular Systems
Eindhoven University of Technology
Den Dolech 2, 5600 MB Eindhoven, The Netherlands

Prof. S. Stallinga
Department of Imaging Physics
Delft University of Technology
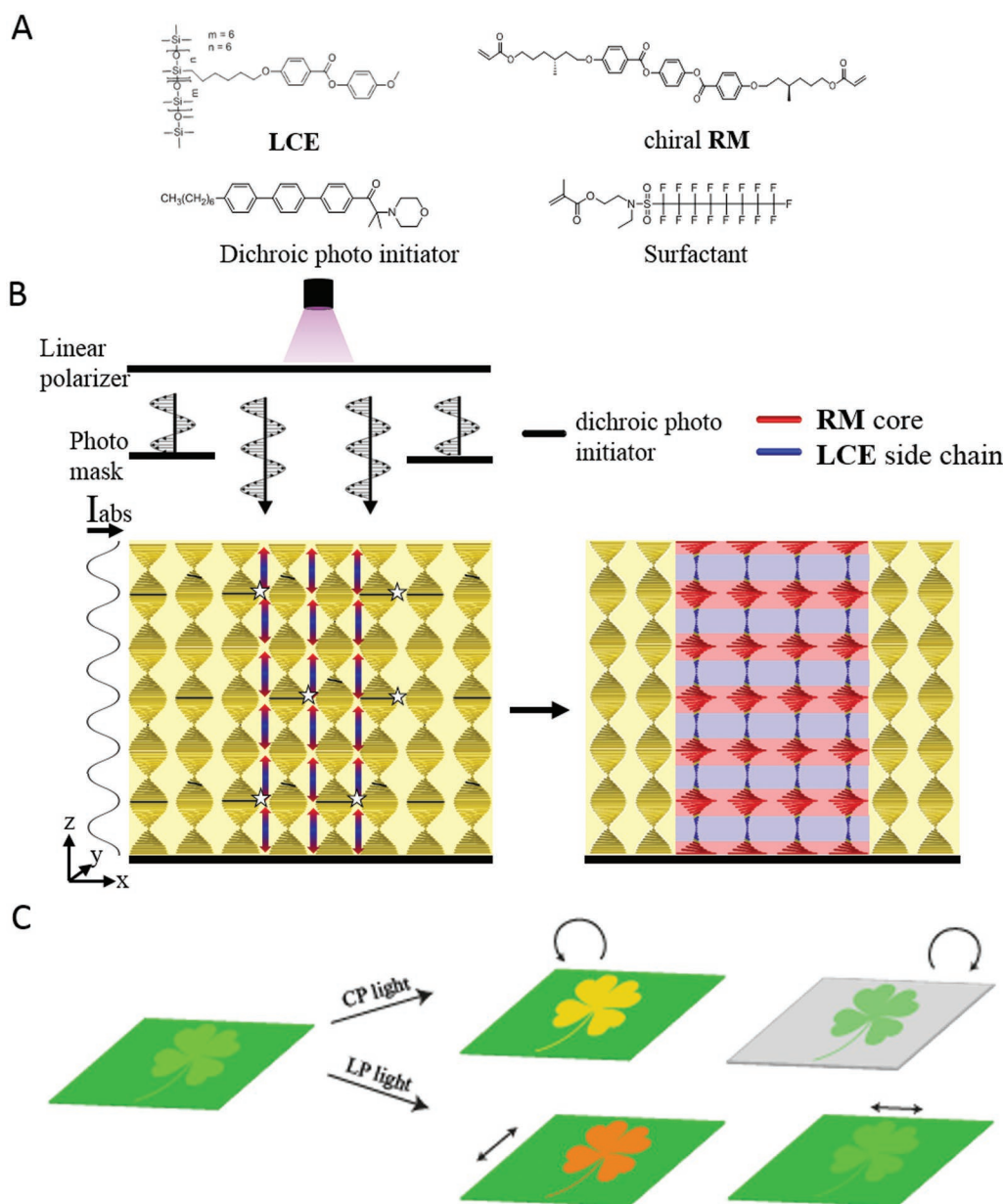Lorentzweg 1, 2628 CJ Delft, The Netherlands

**ADVANCED
SCIENCE NEWS**

www.advancedsciencenews.com

**ADVANCED
MATERIALS**

www.advmat.de

Figure 1. A) Components used in the coating formulation. B) Schematic drawing of the fabrication of 3D helix engineered chiral nematic polymers. Only the areas exposed with LP light are stratified, whereas the nonexposed areas maintain a regular chiral nematic helix. The yellow color indicates homogeneously mixed LCE and RM. For the sake of clarity, the polymer backbones of the LCN and LCE are not drawn. C) The various areas have distinct CP and LP light dependent photonic properties due to which a polarization-dependent decoration of the photomask image (e.g., a clover leaf) can be fabricated.

nonstratified polymer reflects as a regular chiral nematic LC. This results in a polarization-dependent contrast for both circular and linear polarization states of light. By simulations, we found that the photonic properties of the stratified polymers originate from a distorted helical structure. These 3D helix engineered chiral photonic materials show unique linear and circular polarized features making them appealing for applications ranging from security features to super-reflective films.

We prepared chiral nematic LC coating formulations containing siloxane-based LCE, photopolymerizable chiral RM, dichroic photoinitiator (1 wt%), and a surfactant (1 wt%), which ensures alignment of the mixture at the coating–air interface

(**Figure 1**A). LP UV light in combination with the dichroic initiator and a photomask is used to engineer the helical structure of the chiral nematic LC mixture in three dimensions. After application of the mixture using blade coating (coating direction defined at 0°), we illuminated the coating with LP UV light (polarization direction at 90°) through a photomask with the desired image. The dichroic photoinitiator aligns with the periodic helical structure of the chiral nematic LC and preferably absorbs light polarized in the same direction as the molecular orientation. Therefore, polymerization in the exposed areas is mostly initiated when the molecular direction of the initiator is the same as the polarization direction, which is every half a pitch length.[34]

Due to faster consumption of RM in these areas, diffusion of RM toward these areas is induced, thereby creating stratified layers of LCN-rich and LCE-rich material, which alternate with a periodicity equal to the length of half a pitch of the original chiral nematic helix (Figure 1B). The periodic compositional variation of LCN and LCE gives rise to i) a distortion of the helical structure due to localized variation of the chiral dopant concentration and ii) a periodic numerical variation of n_e and n_o (Figure S1, Supporting Information).[32,35] After LP UV light illumination through the photomask, the entire coating is cured with unpolarized UV light. This curing process results in a coating in which the areas illuminated with LP UV light contain a distorted helical structure, whereas the surrounding areas contain a regular chiral nematic LC helix. Due to distinct polarization-dependent photonic properties of these two regions, we could fabricate decorated polymer films with a changing color contrast upon altering the polarization of incident light (Figure 1C).

We first engineered the classic structure of the chiral nematic LC mixture along the helix axis by stratification using LP light in combination with the dichroic photoinitiator. We illuminated about two-third of the coating with LP light (stratified), whereas the remaining part of the coating was only illuminated with unpolarized light (nonstratified). In this experiment, we used a formulation containing 21 wt% chiral RM. The reflection band of the resulting 25 µm thick stratified coating is centered at 677 nm and reflects mostly at the n_o-edge (659 nm, 72%), so that the reflection band has an asymmetric shape (**Figure 2**A). In comparison, the nonstratified region of the coating reflects only 38% of unpolarized light with a symmetric reflection band (Figure 2A,

dashed line). Due to the stratification process, we observe so-called super-reflectivity by exceeding the 50% reflection limit of regular chiral nematic LCs. In addition, the stratified part reflects both handedness of CP light, whereas the nonstratified part reflects only LCP light (Figure 2B). Both regions reflect incoming LCP light effectively, albeit the central reflective wavelength (λ_r) is slightly redshifted for the stratified region with respect to the nonstratified region (687 and 677 nm, respectively). The stratified coating reflects about 70% of incoming right circularly polarized (RCP) light at the n_o-edge of the reflection band (649 nm), which is in line with the asymmetric shape of the unpolarized light spectrum. The coating also shows an LP light dependency of the reflection band with a maximum for light polarized at 45° and a minimum for light polarized at 135° (Figure 2C,D). With LP light at 45°, the coating reflects 85% at the n_o-edge (658 nm) of the reflection band, whereas with LP light at 135°, the coating reflects 60% at the n_e-edge (690 nm), which again is in line with the asymmetric reflection band of the unpolarized light spectrum. Such an LP light dependency is not observed in the nonstratified region of the coating (Figure 2C,D, dashed lines).

By changing the concentration of chiral RM in the coating formulation, λ_r can be tuned between 537 and 927 nm (**Figure 3**A). All the coatings show an asymmetric reflection band with a maximum reflection at the n_o-edge, where they reflect between 66% and 73% of incoming unpolarized light, and showed similar polarization-dependent properties (Figure S2, Supporting Information). For the green and red reflective coatings (25.5 and 21.0 wt% chiral RM, respectively), the intensity difference between the stratified and nonstratified
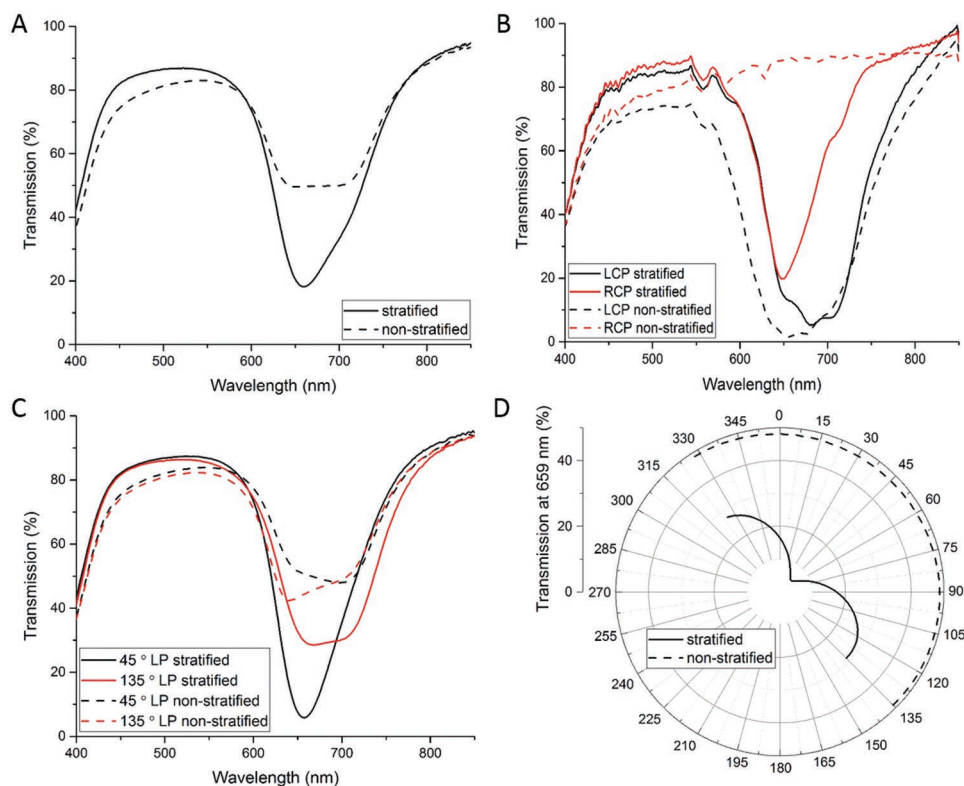

Figure 2. Transmission spectra of the stratified (solid lines) and nonstratified (dashed lines) chiral photonic structures for A) unpolarized light, B) CP light, and C) LP light. D) A polar plot of the transmission at 659 nm.
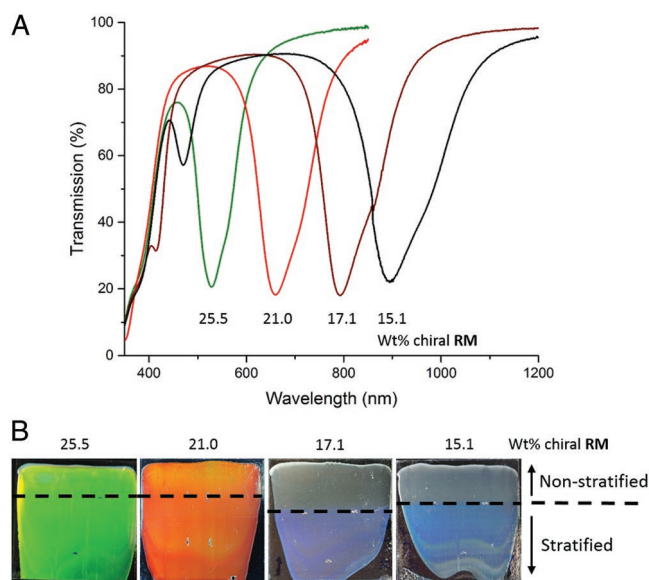
Figure 3. A) Unpolarized light transmission spectra of stratified chiral photonic polymers fabricated from mixtures containing various concentrations of chiral RM. B) Photographs of the various coatings on a black background. Below the dashed lines, the coatings are stratified, whereas above, the coating is nonstratified. The color visible for the stratified part of the coatings reflecting in the near-IR (17.1 and 15.1 wt% chiral RM) originates from the second order reflection peak.

regions of the coating is difficult to detect by the human eye. However, the coatings reflecting in the near-IR region at 818 and 927 nm (17.1 and 15.1 wt% chiral RM, respectively) show a second order reflection peak in the visible light regime (416 nm (visible as purple) and 471 nm (visible as blue), respectively), which makes the stratified and nonstratified regions of the coating clearly distinguishable (Figure 3B).

In addition to the altered reflectivity and polarization dependency of the stratified coatings, the reflectivity demonstrates a dependence on film thickness, which is not seen in the nonstratified chiral photonic coatings for thicknesses >5 µm (Figure S3, Supporting Information). Stratified coatings of 14, 19, and 25 µm reflected 57%, 66%, and 72% of incoming unpolarized light at their lowest point in the transmission curve, respectively. Thinner stratified coatings reflected less RCP and showed a larger LP light dependency. In addition, we found that coatings stratified with LP light parallel to the drawing direction of the coating procedure (0°) showed less enhanced photonic properties, but a similar CP and LP light dependency compared to coatings cured perpendicular to the drawing direction (90°), except that the maximum and minimum LP light reflection are rotated (Figure S4, Supporting Information). The difference in photonic properties between coatings stratified with LP light parallel and perpendicular to the drawing direction might be explained by a shear-induced preferential alignment of the LCE backbone along the coating direction, which hinders diffusion of RM ordered in this direction, resulting in a less pronounced stratification process.

We simulated the structure and the corresponding photonic properties of the stratified chiral photonic materials using an S-matrix method written in MATLAB (Method S1 and File S1,

Supporting Information).[36–41] In the script, we used experimentally obtained values for n_e and n_o (Figure S1, Supporting Information). We tested the script by simulation of a regular chiral nematic LC medium, which resulted in the expected photonic properties (Figure S5, Supporting Information). We simulated three different stratification scenarios; i) one in which the RM accumulates at the center of the high absorption area during the stratification process, ii) one in which the RM distributes homogeneously around the center of this area, and iii) one in which the RM does not reach the center of this area and accumulates around it. We found that only the latter stratification scenario simulated photonic characteristics that match the experimentally observed properties, meaning that the reflection band is enhanced and asymmetric toward the n_o-edge (**Figure 4**). For phase separation scenarios (i) and (ii) the reflection band is also enhanced, but symmetric or asymmetric toward the n_e-edge, respectively (Figures S6 and S7, Supporting Information). The specific stratification scenario in which the RM accumulates around the center of the high absorption areas during the stratification process is thus crucial to obtain the photonic characteristics as found experimentally. Due to the accumulation of RM around the center of high absorption during the stratification process, the helical structure is alternatingly compressed and elongated, due to which it describes an elliptical pathway instead of a circular one as in a conventional chiral nematic liquid crystal. Therefore, it can be rationalized that the stratified photonic structure reflects elliptical polarized light, and thus both handedness of CP light and LP light dependent. In addition, the thickness dependency observed experimentally is also supported by simulation (Figure S8, Supporting Information). Mismatches between simulated and experimental reflection bands might be explained by imperfect planar orientation of the LCs in the experimental sample. This imperfection decreases transmission outside the reflection band and limits the efficiency with which the stratification process can take place and with which the photonic structure can build up constructive interference and thus reflectivity. In addition, during fabrication, the LP curing light might become slightly rotated or elliptically polarized while propagating through the chiral nematic LC medium. It should also be noted that the quarter-wave plate used to generate CP light experimentally is optimized for 532 nm, so that at λ_r of the coating the probing light is somewhat elliptical.

We fabricated a 3D engineered photonic coating (14 µm) using the green reflecting mixture (25.5 wt% chiral RM) by first illuminating the sample with LP light (90°) through a photomask with a clover leaf image (Figure 1B). The entire coating was subsequently cured with unpolarized light. In this way, the clover leaf image contains stratified chiral photonic polymer, whereas the surrounding contains nonstratified chiral photonic polymer. Therefore, the appearance of the clover leaf image is dependent on the polarization state of light (**Figure 5**). With unpolarized light, a minor color difference is visible between the clover leaf and the surrounding area, as the clover leaf reflection band is slightly redshifted compared to the surroundings (λ_r = 557 and 548 nm, respectively) and the n_o-edge (540 nm) of the clover leaf is not as dominant as for a thick coating (Figure S9A, Supporting Information). For LCP light, λ_r of a stratified coating is slightly redshifted with respect to a
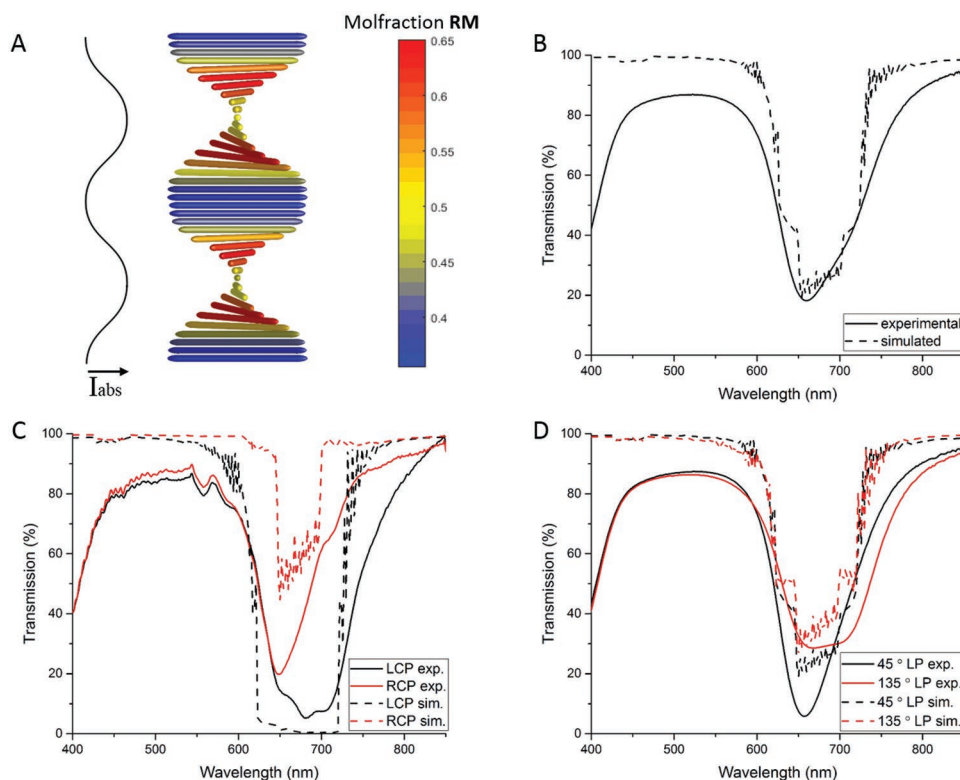
Figure 4. A) Schematic representation of a stratified chiral photonic material along one pitch length in which the chiral RM accumulates around the center of the high absorption areas during the stratification process. The color bar indicates the mole fraction of chiral RM. B–D) Comparison between the simulated and experimental photonic properties of the stratified chiral photonic material for B) unpolarized light, C) CP light, and D) LP light.

nonstratified coating. Therefore, when viewed with LCP light, the clover leaf is visible as orange ($\lambda_r = 562$ nm), whereas the surrounding is still visible as green. With RCP light, the clover leaf reflects at the n_o-edge ($\lambda_r = 541$ nm) and is visible as green, whereas the surrounding area does not reflect, so the black
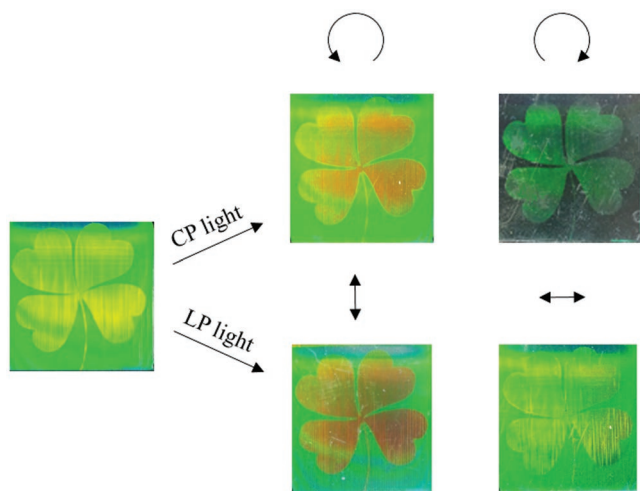

Figure 5. Photographs of a decorated polymer coating viewed with different polarization states of light. The photograph on the left shows the coating viewed with unpolarized light. For the other photographs, the polarization states are indicated by the arrows (top left/right: LCP/RCP light, bottom left/right: 0°/90° LP light).

background becomes visible (Figure S9B, Supporting Information). The clover leaf shows a rotated LP light dependency with respect to the stratified chiral photonic polymers described above (maximum and minimum reflection are at 105° and 15° LP light, Figure S9D, Supporting Information). This can be explained by the birefringence and optical axis of the photomask sheet used, due to which the LP curing light is rotated or even elliptically polarized before it propagates through the coating (Figure S10, Supporting Information). With 0° LP light, the clover leaf is visible as orange, since light is mainly reflected at the n_e-edge (577 nm), whereas the surrounding has no such LP light dependency and still reflects green. With 90° LP light, the clover leaf is also visible as green, since light is mainly reflected at the n_o-edge (538 nm) and becomes almost indistinguishable from the surrounding (Figure S9D, Supporting Information). These results reveal that it is possible to 3D engineer the helical organization in a chiral photonic polymer showing unique polarization-dependent optical changes.

In conclusion, we fabricated polarization-dependent decorated polymers by 3D helix engineering of chiral photonic materials. The helical structure of the polymer is locally distorted by stratification of an LCE and LCN by illumination with LP light through a photomask. Simulations match the experimentally observed optical properties in the stratified areas and reveal a specific stratification profile in which the RM accumulates around the center of the high absorption areas during the stratification process resulting in a specific distortion of the photonic structure. The stratified areas reflect both

1903120 (5 of 7)

handedness of CP light, thereby exceeding the 50% reflection limit for unpolarized light of regular chiral nematic LCs. Furthermore, the stratified chiral photonic polymer reflects both CP and LP light differently than regular chiral nematic LCs, resulting in a changing contrast in color of the decorated polymer coating upon changing the polarization of incoming light. These polarization-dependent decorated polymers have potential to be used in applications where aesthetics and distinctive polarization properties are required, such as security features, but also as reflective optical films where super-reflectivity is needed. The present findings provide a novel method to fabricate bioinspired 3D photonic structured materials with new optical properties.

Experimental Section

Materials: The LCE ((4-methoxyphenyl 4-hexyloxy)benzoate) siloxane) was purchased from Synthon Chemicals GmbH & Co. Chiral RM ((*R*,*R*)-1,4-di-(6-acryloyloxy-3-methylhexyloxy)benzoyloxy) benzene) was obtained from Philips Research lab. The dichroic photoinitiator (1-(4″-heptyl-[1,1′:4′,1″-terphenyl]-4-yl)-2-methyl-2-morpholinopropan-1-one) was obtained from Merck. The surfactant (2-(*N*-ethylperfluorooctanesulfonamide) ethyl methacrylate) was purchased from Acros. Polyimide (Optmer AL 1051) was purchased from JSR Micro.

Rubbed Polyimide Substrates: 3×3 cm^2 glass plates were cleaned, ultrasonicated in ethanol for 30 min, and subsequently treated with UV-Ozone (PR-100, Ultra Violet Products) for 20 min. A polyimide layer was spin-coated on these glass plates using a Karl Suss CT 62 spin coater by rotating at 800 rpm for 5 s, followed by 5000 rpm for 45 s. The polyimide coated glass slides were first placed at 100 °C for 15 min and subsequently at 180 °C for 1.5 h to ensure thermal annealing. The substrates were then rubbed on a velvet cloth.

Mixtures: The components were weighed in the desired ratio and subsequently dissolved in toluene (50 wt%) using a moving plate for at least 1 h.

Refractive Indices Measurements: The refractive indices of various LCE/RM compositions were measured by preparing a series of nematic mixtures of LCE (66.7, 72.3, 77.5, 82.6, and 87.1 wt%), an achiral analogue of RM, namely, 1,4-phenylene bis(4-((6-(acryloyloxy)-hexyl)oxy)benzoate) (RM-82, obtained from Merck; 31.5, 25.3, 20.7, 15.3, and 10.9 wt%, respectively), dichroic photoinitiator (≈1 wt%), and surfactant (1 wt%). The mixtures were uniaxially aligned by filling overnight at ≈55 °C in a 7.7 μm LC cell with planar alignment layers (Instec). The actual thicknesses of the empty cells (*d*) were calculated from the interference pattern of the transmission spectra measured on a Shimadzu UV-3102 PC UV/vis/NIR spectrophotometer, using the formula

$$d = \frac{\lambda_1 \times \lambda_2}{4 \times n_{gap} \times (\lambda_1 - \lambda_2)} \tag{1}$$

in which λ_1 and λ_2 are the wavelengths of two consecutive extrema and n_{gap} is the refractive index of the gap (air, so $n_{gap} = 1$).[42] After filling, the cells were cooled down to 40 °C and left for about 1 h prior to curing at this temperature for 10 min with an intensity of 30 mW cm^{-2} using an EXFO Omnicure S2000. Transmission spectra were measured with LP light parallel and perpendicular to the molecular director, from which n_e and n_o were calculated, respectively. The refractive indices were calculated from the interference patterns of the transmission spectra using the formula

$$n_{e,o} = \frac{m \times \lambda}{2 \times d} \tag{2}$$

in which *m* is the interference order and λ the wavelength at that specific *m*.[43] Using this formula, the refractive index dispersions over the measured wavelength range were calculated, which were then fitted with a two-coefficient Cauchy model

$$n_{e,o} = A + \frac{B}{\lambda^2} \tag{3}$$

in which *A* and *B* are fitting constants.[44] Using this fit, the refractive indices at 677 nm were measured, which was the center of the reflection band of the red reflecting stratified chiral photonic polymer. For the calculations, *m* was chosen such that the refractive index values are in the order range of values reported in literature.[45] In addition, the birefringence ($n_e - n_o$) was verified using a Leica CTR6000 polarized optical microscope, which was equipped with a compensator crystal (Leica Tilting Compensator K).

Coating Preparation and Stratification Process: Coatings were prepared using an RK PrintCoat Instruments K control coater. Mixtures were applied on a rubbed polyimide substrate and placed at 100 °C for ≈35 min to evaporate the solvent. When the mixtures turned completely white at room temperature, it was assumed that all solvent was evaporated. For the application of the mixtures, the 10 μm gap of a 4-sided applicator (10–25 μm gaps, ZFR 2040, Zehntner) was used, which was automatically pushed forward over the mixture. The speed was varied between ≈1 and 1.5 cm s^{-1} to tune the coating thickness. The coating was placed in a nitrogen box at 40 °C and a high contrast linear polarizer was placed for UV (PUVD260C35S from LOT-QuantumDesign GmbH) above the coating to cover approximately two-third of the coating. The coating was illuminated with an energy dose of ≈275 mJ cm^{-2} (8.3 mW cm^{-2} for 33.1 s) using an EXFO Omnicure S2000 mercury lamp. The LP light direction was perpendicular (defined as 90°) to the coating direction (defined as 0°), unless specified otherwise. Subsequently, after waiting for 1 min during which the linear polarizer was removed, the coating was post cured for 10 min with a high UV intensity of ≈25 mW cm^{-2}.

Decorated Coatings: Decorated coatings were prepared in a similar way as described above, except that a photomask was placed above the coating during the illumination step with LP light. The photomask was fabricated by printing a clover leaf image on a transparent overhead sheet three times, which ensured blocking most of the light (>99%) in the printed areas.

Vis–NIR Transmission Spectra: Transmission spectra of the coatings for unpolarized light were measured at a Perkin Elmer Lambda 750 UV/vis/NIR spectrophotometer. For LP light transmission spectra and polar plots, this spectrophotometer was equipped with a linear polarizer. Transmission spectra with CP light were measured on a Shimadzu UV-3102 PC equipped with a linear polarizer in combination with a quarter-wave plate.

Supporting Information

Supporting Information is available from the Wiley Online Library or from the author.

Acknowledgements

**ADVANCED
SCIENCE NEWS**
www.advancedsciencenews.com

**ADVANCED
MATERIALS**
www.advmat.de

[1] V. Sharma, M. Crne, J. O. Park, M. Srinivasarao, *Science* **2009**, *325*, 449.
[2] P. Vukusic, J. R. Sambles, *Nature* **2003**, *424*, 852.
[3] S. Tadepalli, J. M. Slocik, M. K. Gupta, R. R. Naik, S. Singamaneni, *Chem. Rev.* **2017**, *117*, 12705.
[4] J. Sun, B. Bhushan, J. Tong, *RSC Adv.* **2013**, *3*, 14862.
[5] L. P. Biró, J. P. Vigneron, *Laser Photonics Rev.* **2011**, *5*, 27.
[6] F. P. Barrows, M. H. Bartl, *Nanomater. Nanotechnol.* **2014**, *4*, 1.
[7] X. Wu, F. L. Rodríguez-Gallegos, M. C. Heep, B. Schwind, G. Li, H. O. Fabritius, G. von Freymann, J. Förstner, *Adv. Opt. Mater.* **2018**, *6*, 1800635.
[8] T. Lu, W. Peng, S. Zhu, D. Zhang, *Nanotechnology* **2016**, *27*, 1.
[9] S. A. Jewell, P. Vukusic, N. W. Roberts, *New J. Phys.* **2007**, *9*, 99.
[10] M. Kolle, P. M. Salgard-Cunha, M. R. J. Scherer, F. Huang, P. Vukusic, S. Mahajan, J. J. Baumberg, U. Steiner, *Nat. Nanotechnol.* **2010**, *5*, 511.
[11] X. Qing, Y. Liu, J. Wei, R. Zheng, C. Zhu, Y. Yu, *Adv. Opt. Mater.* **2019**, *7*, 1801494.
[12] Y. Wang, W. Li, M. Li, S. Zhao, F. De Ferrari, M. Liscidini, F. G. Omenetto, *Adv. Mater.* **2019**, *31*, 1.
[13] J. Hou, M. Li, Y. Song, *Angew. Chem., Int. Ed.* **2018**, *57*, 2544.
[14] A. Ryabchun, O. Sakhno, J. Stumpe, A. Bobrovsky, *Adv. Opt. Mater.* **2017**, *5*, 1700314.
[15] Q. Li, Y. Li, J. Ma, D. K. Yang, T. J. White, T. J. Bunning, *Adv. Mater.* **2011**, *23*, 5069.
[16] A. Benedetti, B. Alam, M. Esposito, V. Tasco, G. Leahu, A. Belardini, R. Li Voti, A. Passaseo, C. Sibilia, *Sci. Rep.* **2017**, *7*, 1.
[17] T. D. Nguyen, M. J. MacLachlan, *Adv. Opt. Mater.* **2019**, *7*, 1801275.
[18] J. A. Dolan, B. D. Wilts, S. Vignolini, J. J. Baumberg, U. Steiner, T. D. Wilkinson, *Adv. Opt. Mater.* **2015**, *3*, 12.
[19] M. Saba, M. Thiel, M. D. Turner, S. T. Hyde, M. Gu, K. Grosse-Brauckmann, D. N. Neshev, K. Mecke, G. E. Schröder-Turk, *Phys. Rev. Lett.* **2011**, *106*, 1.
[20] M. D. Turner, M. Saba, Q. Zhang, B. P. Cumming, G. E. Schröder-Turk, M. Gu, *Nat. Photonics* **2013**, *7*, 801.
[21] V. A. Belyakov, V. E. Dmitrienko, V. P. Orlov, *Phys.-Usp.* **1979**, *22*, 64.
[22] I. Dierking, *Symmetry* **2014**, *6*, 444.
[23] G. Chilaya, in *Chirality in Liquid Crystals* (Eds: H. Kitzerow, C. Bahr), Springer-Verlag, New York **2001**, pp. 159–185.
[24] M. Mitov, *Adv. Mater.* **2012**, *24*, 6260.
[25] M. Mitov, N. Dessaud, *Liq. Cryst.* **2007**, *34*, 183.
[26] N. Katsonis, E. Lacaze, A. Ferrarini, *J. Mater. Chem.* **2012**, *22*, 7088.
[27] M. E. McConney, V. P. Tondiglia, J. M. Hurtubise, L. V. Natarajan, T. J. White, T. J. Bunning, *Adv. Mater.* **2011**, *23*, 1453.
[28] G. Chen, L. Wang, Q. Wang, J. Sun, P. Song, X. Chen, X. Liu, S. Guan, X. Zhang, L. Wang, H. Yang, H. Yu, *ACS Appl. Mater. Interfaces* **2014**, *6*, 1380.
[29] Y. Zhao, L. Zhang, Z. He, G. Chen, D. Wang, H. Zhang, H. Yang, *Liq. Cryst.* **2015**, *42*, 1120.
[30] H. Khandelwal, R. C. G. M. Loonen, J. L. M. Hensen, A. P. H. J. Schenning, M. G. Debije, *J. Mater. Chem. A* **2014**, *2*, 14622.
[31] Y. Li, Y. J. Liu, H. T. Dai, X. H. Zhang, D. Luo, X. W. Sun, *J. Mater. Chem. C* **2017**, *5*, 10828.
[32] D. J. Broer, *Curr. Opin. Solid State Mater. Sci.* **2002**, *6*, 553.
[33] A. J. J. Kragt, D. J. Broer, A. P. H. J. Schenning, *Adv. Funct. Mater.* **2018**, *28*, 1704756.
[34] D. J. Broer, G. N. Mol, J. A. M. M. Van Haaren, J. Lub, *Adv. Mater.* **1999**, *11*, 573.
[35] B. Serrano-ramón, C. Kjellander, S. Zakerhamidi, C. W. M. Bastiaansen, D. J. Broer, *Proc. SPIE* **2008**, *6911*, 1.
[36] D. W. Berreman, *J. Opt. Soc. Am.* **1972**, *62*, 502.
[37] D. Y. K. Ko, J. R. Sambles, *J. Opt. Soc. Am. A* **1988**, *5*, 1863.
[38] K. Eidner, *J. Opt. Soc. Am. A* **1989**, *6*, 1657.
[39] C. Oldano, *Phys. Rev. A* **1989**, *40*, 6014.
[40] M. A. Christou, N. C. Papanicolaou, C. Polycarpou, *Phys. Rev. E* **2012**, *85*, 031702.
[41] S. Relaix, M. Pevnyi, W. Cao, P. Palffy-Muhoray, *Photonics Res.* **2013**, *1*, 58.
[42] F. Bruyneel, *Opt. Eng.* **2001**, *40*, 259.
[43] E. Miszczyk, Z. Raszewski, J. Kędzierski, E. Nowinowski-Kruszelnicki, M. A. Kojdecki, P. Perkowski, W. Piecek, M. Olifierczuk, *Mol. Cryst. Liq. Cryst.* **2011**, *544*, 22/[1010].
[44] J. Li, C. H. Wen, S. Gauza, R. Lu, S. T. Wu, *J. Disp. Technol.* **2005**, *1*, 51.
[45] D. Liu, D. J. Broer, *Langmuir* **2014**, *30*, 13499.